Electronic Supplementary Material (ESI) for CrystEngComm.

Electronic Supporting Information

Facile synthesis of porous PdCu nanoboxes for efficient chromium (VI) reduction

Bin Qiao,[a] Jingyi Zhu,[a] Yanping Liu,[a] Yu Chen,[a] Gengtao Fu*[b] and Pei Chen*[a]

[a] Key Laboratory of Applied Surface and Colloid Chemistry (MOF), Key Laboratory of Macromolecular Science of Shaanxi Province, School of Materials Science and Engineering, Shaanxi Normal University, Xi'an, 710062, PR China.

[b] School of Chemical and Biomedical Engineering, Nanyang Technological University, Singapore 637459, Singapore

* Corresponding authors.

E-mail addresses: chenpei@snnu.edu.cn (P. Chen); gengtaofu@gmail.com (G. Fu).

Experimental

Reagents and Chemicals

Potassium chloropalladite (II) (K_2PdCl_4) was purchased from Beijing HWRK chem Co., Ltd (Beijing, China). Potassium dichromate ($K_2Cr_2O_7$) and poly(acrylic acid sodium salt) (PAAs, weight-average molecular weight 5000) were purchased from Sigma-Aldrich (Shanghai, China). Copper(II) chloride dihydrate ($CuCl_2{\cdot}H_2O$), potassium hydroxide (KOH), sodium hydroxide (NaOH), ammonia solution ($NH_3{\cdot}H_2O$, 28%), formic acid (HCOOH, 96%) and L-Ascorbic acid (AA) were purchased from Sinopharm Chemical Reagent Co., Ltd (Shanghai, China). Commercial Pd black from Johnson Matthey were purchased from Shanghai Hesen electrical corporation (Shanghai, China). All chemical reagents were of analytical reagent grade and used without further purification.

Instruments

Scanning electron microscopy (SEM) images and energy dispersive X-ray analysis (EDX) were taken on a model SU-8020 instrument. Transmission electron microscopy (TEM) images, high-resolution TEM (HRTEM) images were taken by a JEM-2100 transmission electron microscope operated at an accelerating voltage of 200 kV. X-ray photoelectron spectroscopy (XPS) measurements were tested on AXIS ULTRA spectrometer. The C1s peak energy of 284.5 eV was used as the calibration of binding energy data. X-ray diffraction (XRD) patterns were performed on a DX-2700 X-ray diffractometer with Cu Ka radiation source (λ = 0.15418 nm) and operating at 40 kV and 30 mA. Ultraviolet and visible spectroscopy (UV−vis) data were performed with UV-2600 spectrophotometer.

Synthesis of Cu_2O nanocubes

Typically, 1.0 mL 0.5 M PAAs solution and 2 mL 0.05 M $CuCl_2$ solution were first injected into 30 mL ultrapure water, successively. After stirred for 2 min, 2 mL 0.5 M KOH solution was mixed with 0.6 mL 0.5 M AA solution and diluted with water to 7 mL, followed was slowly dropping into the above solution under continuous stirring, and stirring for 30 min at room temperature. After the reaction, the orange samples were obtained by ultrasonication three times with ultrapure water and ethanol respectively, before vacuum drying at 60 ^oC for 12 hours to obtain the Cu_2O nanocubes.

Synthesis of bimetallic PdCu nanoboxes

Typically, the 6.0 mg Cu_2O nanocubes were dissolved in 30 mL ultrapure water, followed by the injection of 0.5 mL 0.5 M PAAs solution under stirring. After adjusting pH to 11 by 0.1 M KOH, 0.3 mL 0.05 M

K_2PdCl_4 solution was injected into the above mixture under continuous stirring. The mixture was put into a stainless-steel kettle with a polytetrafluoroethylene liner, and was subsequently heated at 120 ^oC for 6 hours. After reaction, the unreacted Cu_2O template in the solution was removed by 5 mL ammonia solution ($NH_3 \cdot H_2O$, 28%). Finally, the PdCu nanoboxes were obtained by centrifugation three times with ultrapure water and ethanol respectively before vacuum drying at 60 ^oC for 12 hours.

Synthesis of solid PdCu nanoparticles

To solid PdCu nanoparticles, we use $NaBH_4$ to directly reduce K_2PdCl_4 and $CuCl_2$ in aqueous solution. Typically, 0.45 mL 0.05 M K_2PdCl_4 solution and 0.55 mL 0.05 M $CuCl_2$ solution were injected into 10 mL ultrapure water at room temperature, then 200 mg $NaBH_4$ was introduced into the mixture solution under strong stirring for 2 hours. Vacuum drying at 60 ^oC for 12 hours after ultrasonic washing with water and ethanol.

Catalytic reduction of Cr(VI)

All photochemical tests were performed on an ultraviolet and visible (UV−vis) spectroscopy. A mixture containing ultrapure water (3 mL), $K_2Cr_2O_7$ (10 μL, 0.2 M), HCOOH (50 μL, 96%), catalyst (2 mg/mL) was taken into cuvette in the UV-vis spectroscopy at room temperature. At each predetermined time, the relationship can be monitored between wavelength and absorbance by the UV-vis spectroscopy. The kinetic rate constant (k) of catalysts can be quantitatively evaluated by following Equation (1) ($\ln(C_t/C_0) = -kt$),[1-3] where C_0 and C_t are the concentrations of Cr(VI) at t = 0 and time t, respectively. According to the relationship between reaction rate constants (k) and temperature (T) in the Arrhenius equation, the activation energy of chemical reaction can be calculated, which was calculated as Equation (2):[4, 5]

$$\mathrm{Ln}\, k = -Ea / (RT) + \mathrm{Ln}A \qquad (2)$$

Where k is the reaction rate constants at different temperature T(K), R is the Molar gas constant (8.314 J/K·mol) and A is the pre-exponential factor.

Experimental Data

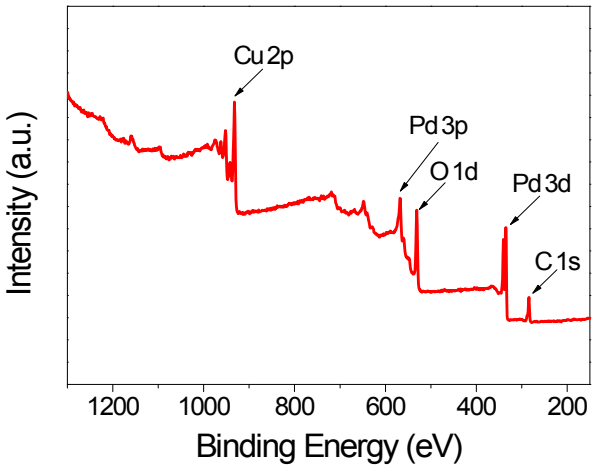

Fig. S1 XPS survey scan spectrum of PdCu nanoboxes.

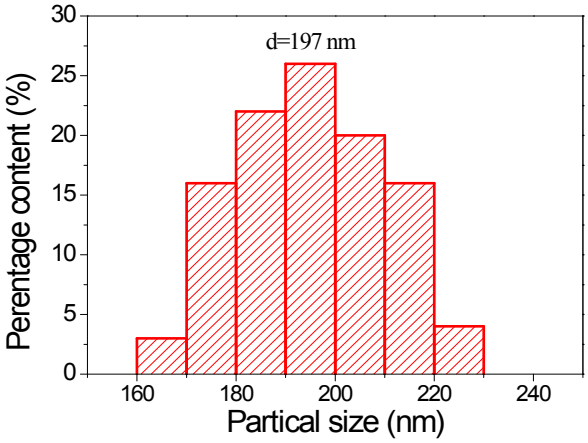

Fig. S2 The corresponding particle-size distribution histogram of Cu_2O nanocubes.

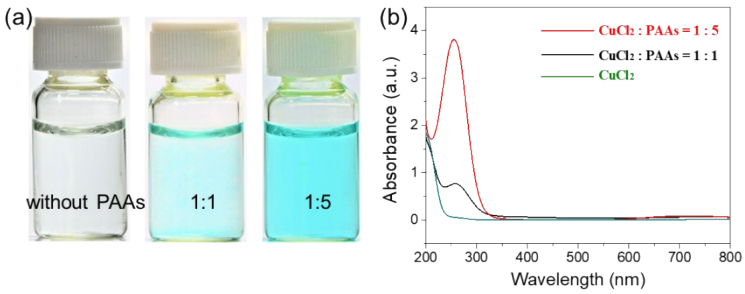

Fig. S3 (a) Optical photos and (b) UV-vis spectra of $CuCl_2$-PAAs mixture with different $CuCl_2$/PAAs ratios: (a) without PAAs; (b) $CuCl_2$: PAAs=1:1; (c) $CuCl_2$: PAAs=1:5.

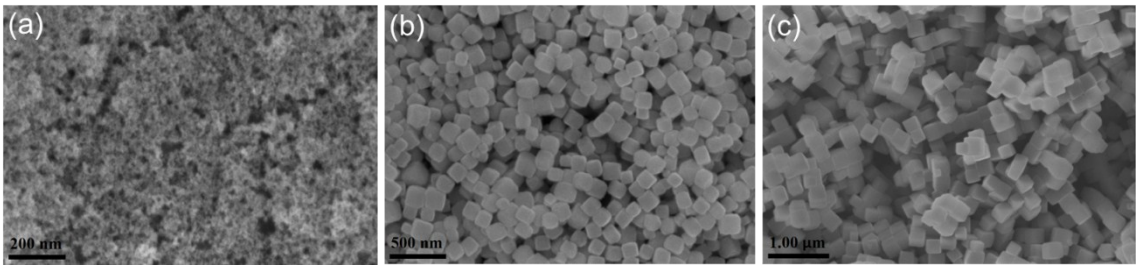

Fig. S4 SEM images of Cu_2O nanocrystals with different $CuCl_2$/PAAs ratios: (a) without PAAs; (b) $CuCl_2$: PAAs=1:1; (c) $CuCl_2$: PAAs=1:5.

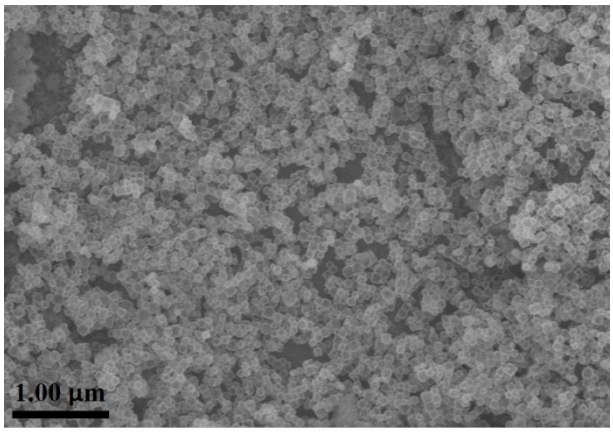

Fig. S5 (a) Large-area SEM images of porous PdCu nanoboxes.

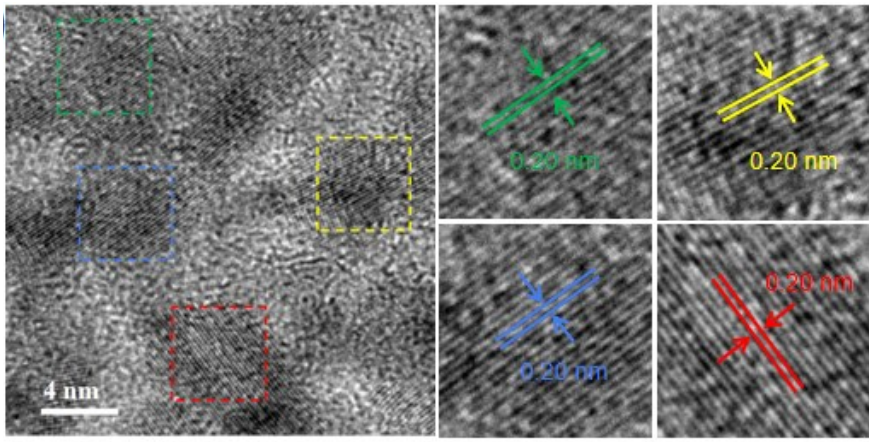

Fig. S6 HRTEM images of PdCu nanoboxes at different lattice directions.

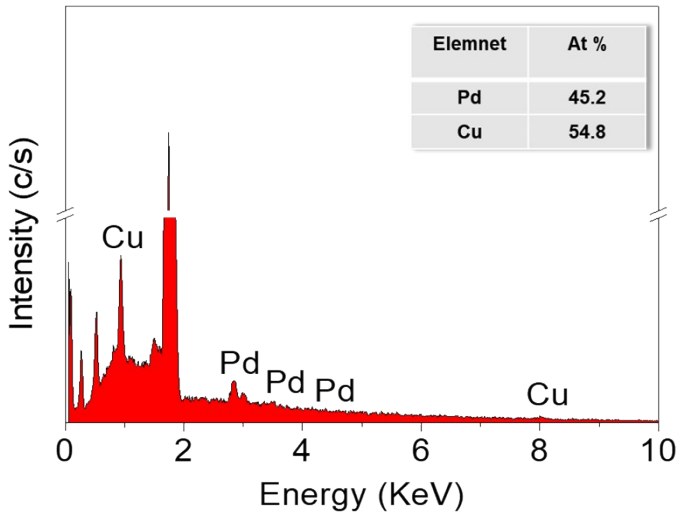

Fig. S7 EDX spectrum of PdCu nanoboxes.

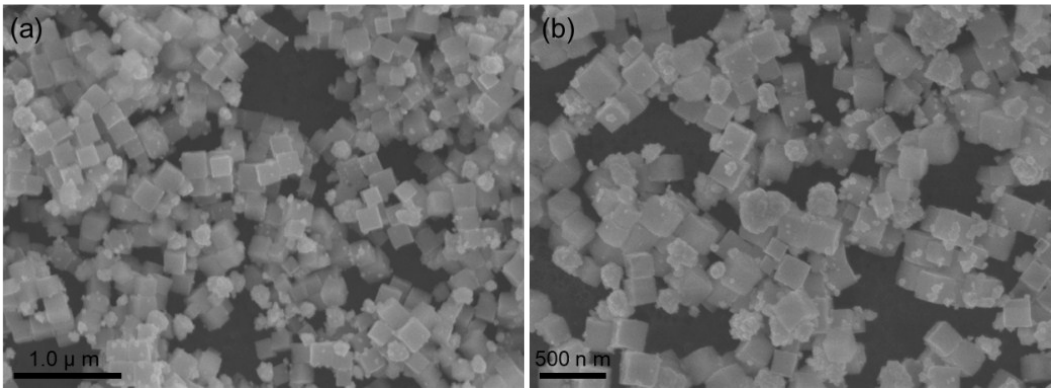

Fig. S8 SEM images of Cu_2O@PdCu in the absence of PAAs.

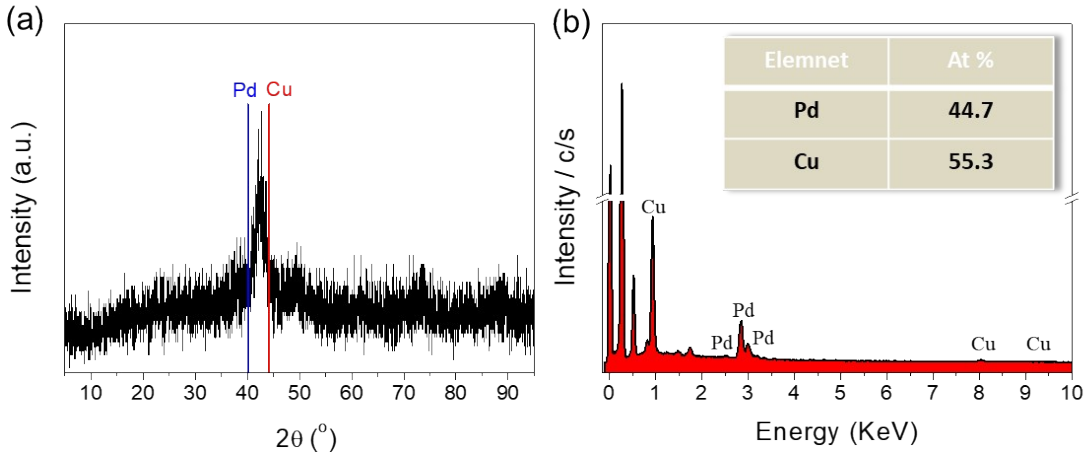

Fig. S9 (a) XRD pattern and (b) EDX spectrum of solid PdCu nanoparticles.

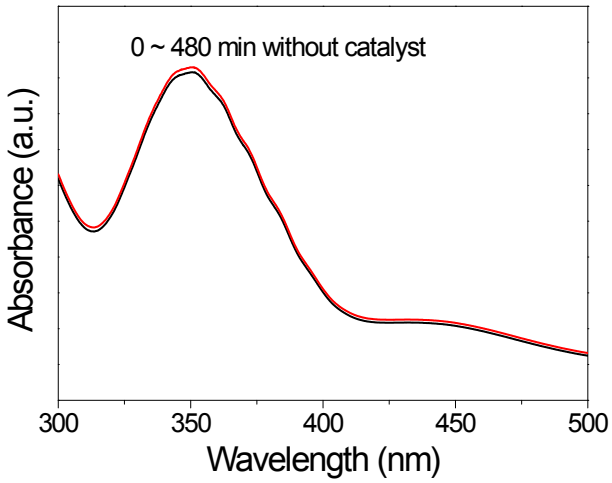

Fig. S10 UV-vis spectrum for the reduction of Cr (VI) without catalyst at 25 ^{o}C.

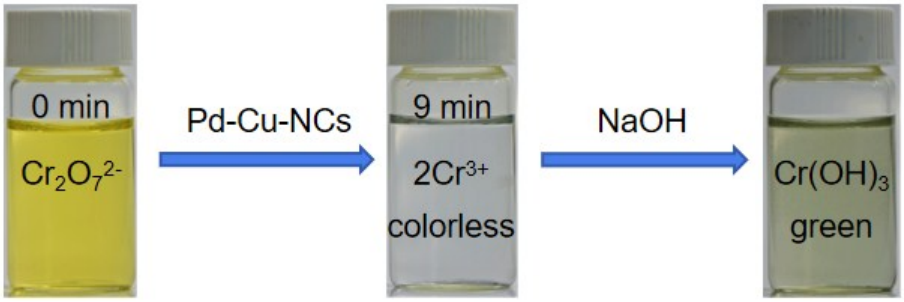

Fig. S11 Photographs of Cr (VI) solution, Cr (III) solution and after adding the excess NaOH.

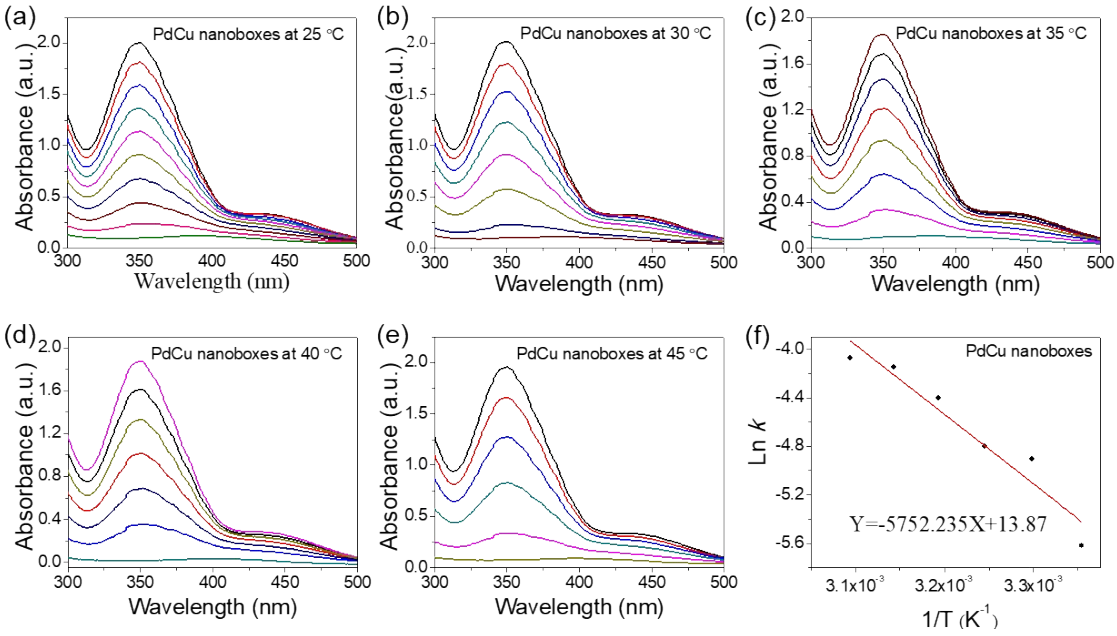

Fig. S12 Time-dependent UV-vis spectra for the reduction of Cr (VI) on PdCu nanoboxes at different temperatures: (a) 25 °C, (b) 30 °C, (c) 35 °C, (d) 40 °C, (e) 45 °C; (f) plots of Ln *k* and 1/T of the Cr(VI) reduction.

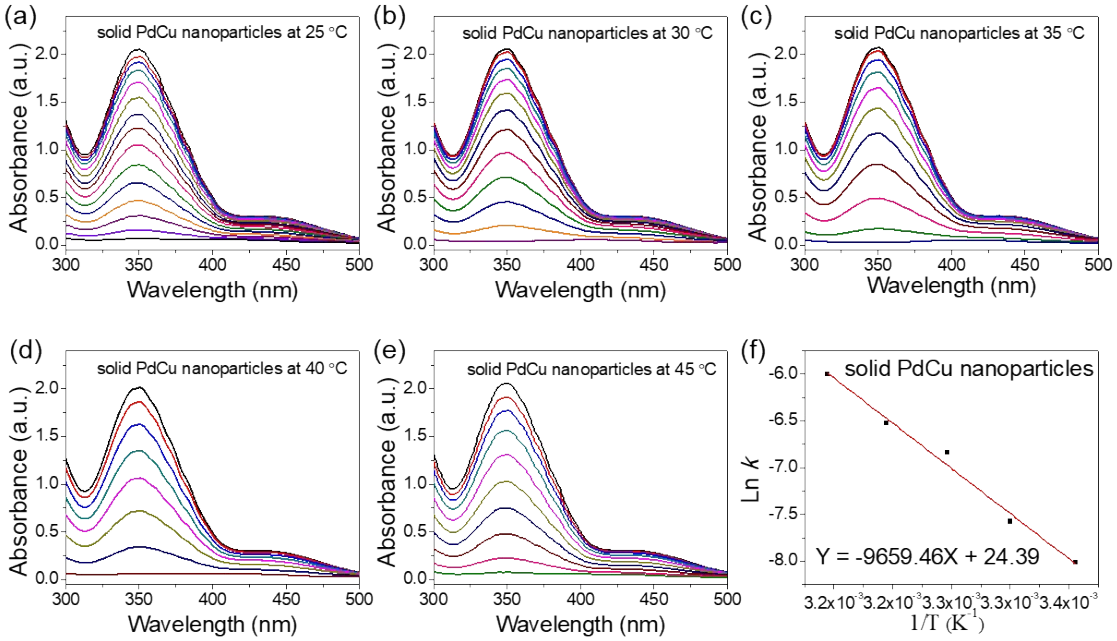

Fig. S13 Time-dependent UV-vis spectra for the reduction of Cr (VI) on solid PdCu nanoparticles at different temperatures: (a) 25 °C, (b) 30 °C, (c) 35 °C, (d) 40 °C, (e) 45 °C; (f) plots of Ln *k* and 1/T of the Cr(VI) reduction.

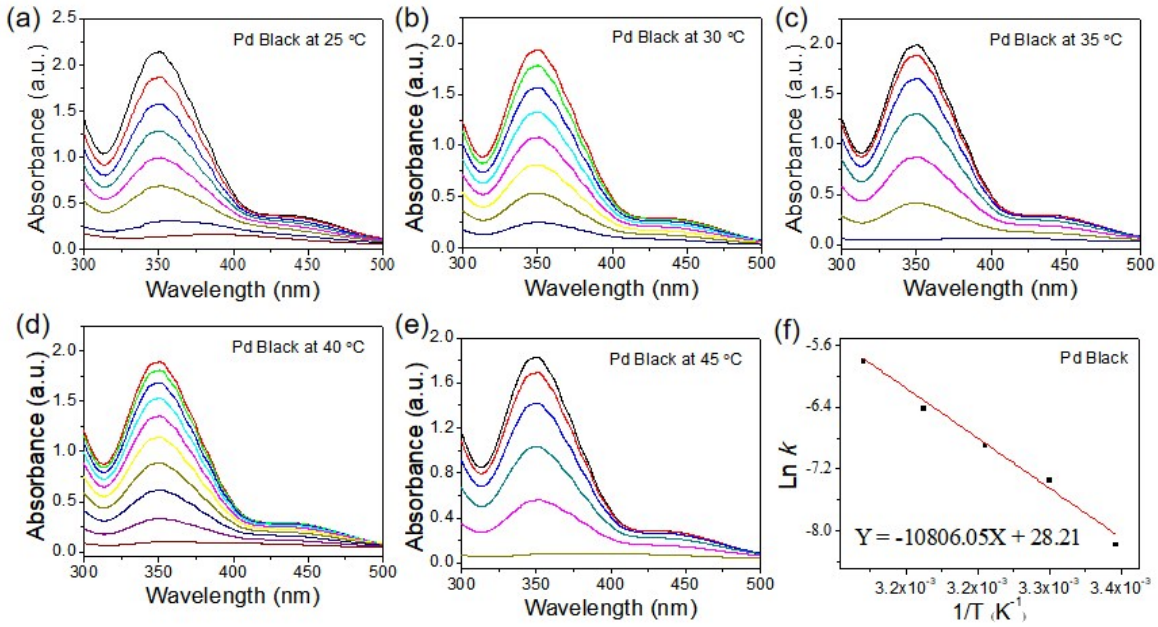

Fig. S14 Time-dependent UV-vis spectra for the reduction of Cr (VI) on Pd Black at different temperatures: (a) 25 °C, (b) 30 °C, (c) 35 °C, (d) 40 °C, (e) 45 °C; (f) plots of Ln *k* and 1/T of the Cr(VI) reduction.

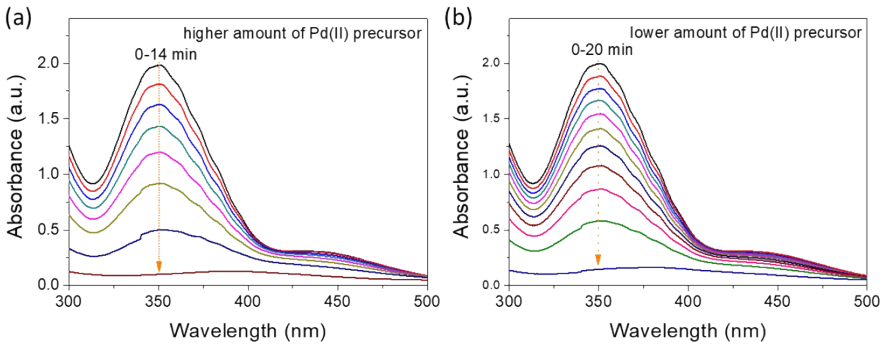

Fig. S15 Time-dependent UV-vis spectra for the reduction of Cr (VI) on PdCu nanocrystals prepared at (a) higher amount of Pd(II) precursor and (b) lower amount of Pd(II) precursor.

***Table S1**. The performance comparisons of PdCu nanoboxes with those of previous-reported Pd-based materials.*

Catalysts	Cycle efficiency (cycle)	k (min^{-1})	Ref.
PdCu Nanoboxes	93.3% (10)	0.274	This work
Pd NPs@pro-ESM	91% (4)	0.133	[6]
Pd@SiO_2–NH_2	85% (5)	0.165	[7]
Pd/bentonite	91% (5)	/	[8]
Pd-CNTs	66% (10)	0.310	[9]
Pd_{urc}	93% (6)	0.067	[10]
Pd/Fe-NMC	75%	0.154	[11]

References

1. G.-T. Fu, X. Jiang, R. Wu, S.-H. Wei, D.-M. Sun, Y.-W. Tang, T.-H. Lu and Y. Chen, *ACS Applied Materials & Interfaces*, 2014, **6**, 22790-22795.

2. S.-H. Han, J. Bai, H.-M. Liu, J.-H. Zeng, J.-X. Jiang, Y. Chen and J.-M. Lee, *Acs Applied Materials & Interfaces*, 2016, **8**, 30948-30955.

3. D.-N. Li, F.-Q. Shao, J.-J. Feng, J. Wei, Q.-L. Zhang and A.-J. Wang, *Materials Chemistry and Physics*, 2018, **205**, 64-71.

4. M. Grigiante, M. Brighenti and D. Antolini, *Journal of Thermal Analysis and Calorimetry*, 2017, **129**, 553-565.

5. C. P. Lin and C. M. Shu, *Journal of Thermal Analysis and Calorimetry*, 2009, **95**, 547-552.

6. M. Liang, R. Su, W. Qi, Y. Zhang, R. Huang, Y. Yu, L. Wang and Z. He, *Industrial & Engineering Chemistry Research*, 2014, **53**, 13635-13643.

7. M. Celebi, M. Yurderi, A. Bulut, M. Kaya and M. Zahmakiran, *Applied Catalysis B-Environmental*, 2016, **180**, 53-64.

8. M. Nasrollahzadeh, S. M. Sajadi, M. Maham and I. Kohsari, *Microporous And Mesoporous Materials*, 2018, **271**, 128-137.

9. J. D. Kim and H. C. Choi, *Bulletin Of the Korean Chemical Society*, 2016, **37**, 744-747.

10. U. S. Markad, A. M. Kalekar, D. B. Naik, K. K. K. Sharma, K. J. Kshirasagar and G. K. Sharma, *Journal Of Photochemistry And Photobiology a-Chemistry*, 2017, **338**, 115-122.

11. S. Li, L. Tang, G. Zeng, J. Wang, Y. Deng, J. Wang, Z. Xie and Y. Zhou, *Environmental Science And Pollution Research*, 2016, **23**, 22027-22036.